FAST PHOTOTHERMAL INSPECTION OF PLASMA-SPRAYED COATINGS OF PRIMARY CIRCULATION SEAL RINGS OF A NUCLEAR REACTOR

R. Lehtiniemi, J. Hartikainen, J. Rantala, J. Varis, and M. Luukkala

University of Helsinki, Department of Physics
Siltavuorenpenger 20 D, SF-00170 Helsinki, Finland

INTRODUCTION

A need for NDE of plasma-sprayed coatings has been a serious problem in the industry for a long time. Traditional methods like ultrasonics or x-ray absorption usually cannot be used because of the high attenuation and the heterogeneity of the coating. On the other hand, sub-surface flaws cannot be detected with liquid penetration technique and electromagnetic methods are not suitable for dielectric coating. However, photothermal techniques have been successfully applied [1,2], but first the introduction of fast infrared scanning systems has lead to reasonable speed of inspection from the practical point of view.

New NDE techniques are likely to be applied first in applications where new materials are introduced and reliability is most important, like in aerospace and nuclear industries. Besides the safety questions also the economical circumstances must be considered. For instance, the failure of nuclear reactor primary circulation seals would cause a stop of the reactor unit and thus substantial financial losses.

SIMULATIONS FOR OPTIMIZING THE MEASUREMENT PARAMETERS

The principle of the applied scanning photothermal evaluation technique is shown in Fig. 1. The sample under inspection is heated by a scanning laser beam focussed on a line and the increased thermal radiation from the sample surface is monitored with an infrared line scanner. Possible delamination defects affect the surface temperature and can thus be detected.

The kind of a situation can be modeled with a computational technique similar to the method previously used to simulate laser heating for crack inspection [3] and delamination detection [4]. Thus, a few computer simulations were performed in order to optimize measurement parameters. Most interesting of these parameters are the least detectable thermal contact resistance caused by the delamination of the coating, the optimum scanning speed, and the optimum distance between the heating and the detection points.

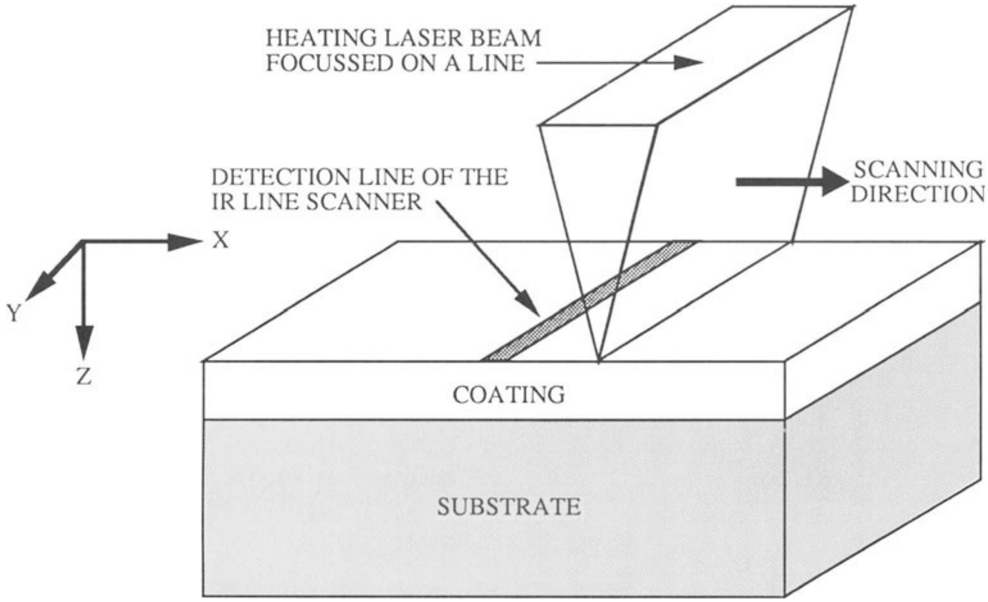

Fig 1. A diagram of the measurement principle.

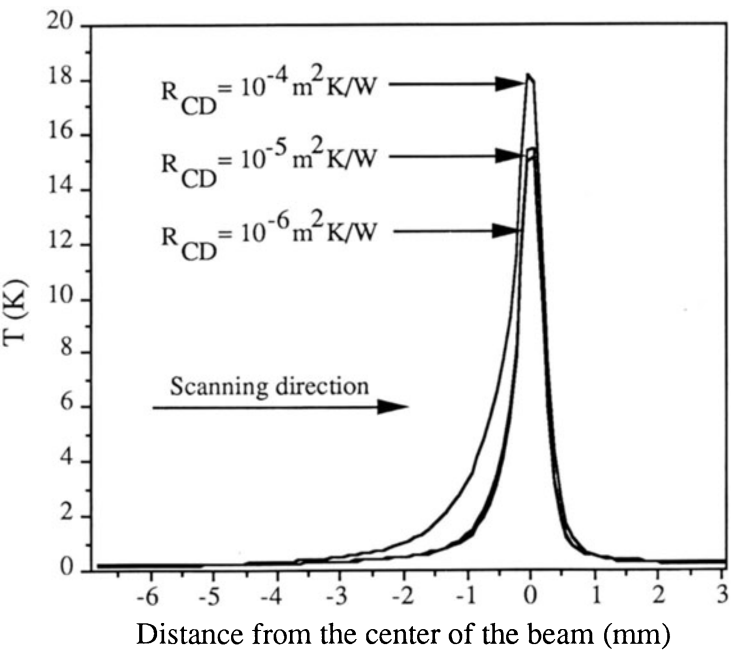

Fig. 2. The instantaneous surface temperature profile due to the scanning heating with different values of thermal contact resistances.

The sample was described with 7-point 3-dimensional molecule model and the resulting time-dependent three-dimensional diffusion equations were solved using Crank-Nicolson and implicit finite difference methods. The material parameters used in the simulations are listed in Table 1.

As an example of the simulations, in Fig. 2 is depicted the surface temperature rise caused by scanning heating with different values of contact resistances and in Fig. 3 the temperature difference between the delaminated and the faultless area in order to determine the optimum distance between the heating and detection points.

The beam 1/3 beam radius used in the simulations was 300 μm and the scanning speed was 2 mm/s. This speed was selected with the help of the simulations as a reasonable compromise. On the other hand, the scanning must be fast enough to maintain reasonable inspection time and on the other hand, the heating time per point must be long enough to produce reasonable quantity of heat.

The contact resistance of order 10-5 m^2K/W is near the limit of detectability. The optimum distance of heating and detecting points is about one fourth of a millimeter when detecting a decade greater contact resistances. In this case the rise of the surface temperature above the defective area is almost four centigrades and clearly detectable.

Table 1. The material parameters of the sample used in the calculations.

Layer	ρ (kg/m^3)	K (W/K · m)	c(J/kg · K)
Coating	5210	2.3	781
Substrate	7860	60	450

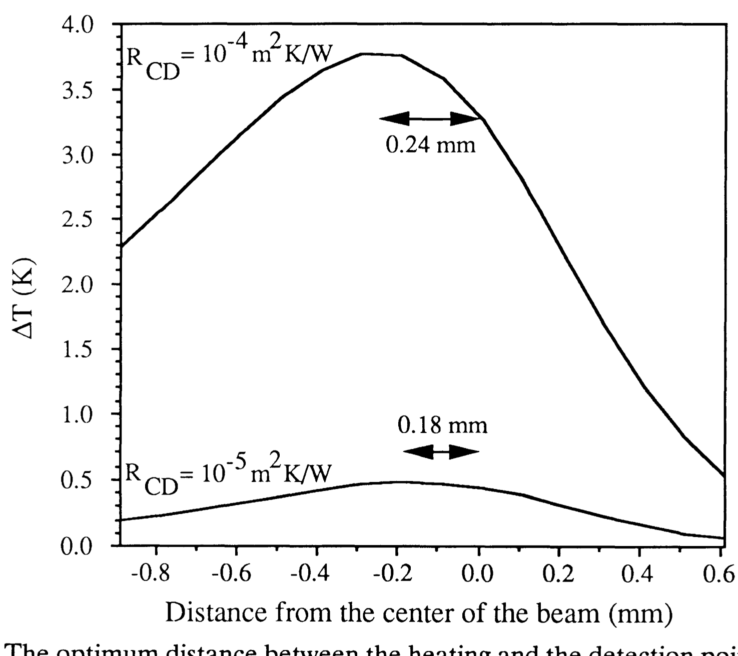

Fig. 3. The optimum distance between the heating and the detection points. ΔT is the temperature difference between the delaminated and the faultless areas.

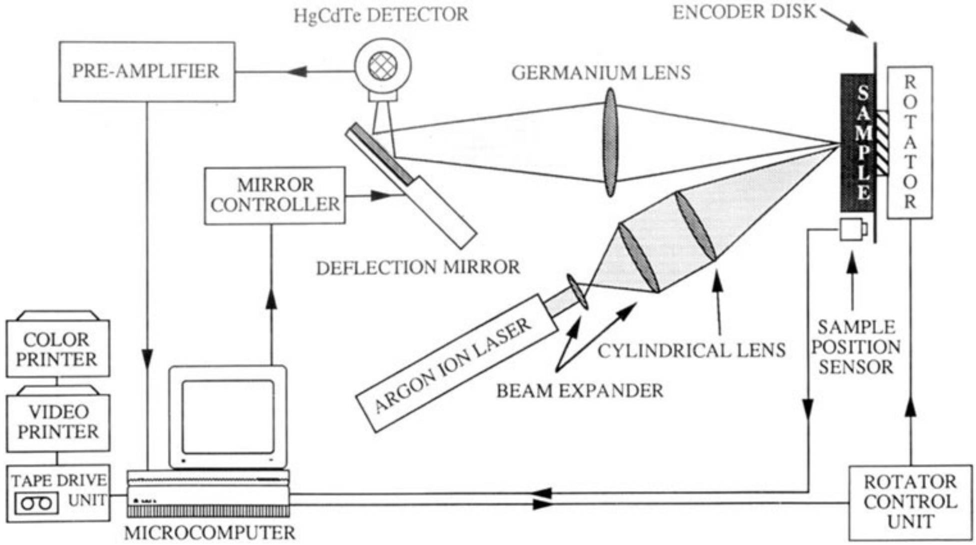

Fig. 4. A schematic diagram of the measurement system.

THE MEASUREMENT SYSTEM

The sample is a pair of axis seal rings of a primary circulation main pump of a nuclear reactor. The rings are made of austenite steel AISI 316 and coated with 300 µm thick plasma-sprayed chromium oxide layer in order to increase the resistance to mechanical strain. The outer diameter of the ring is approximately 30 cm, the height 6 cm and the width of the coated area to be inspected 4 cm.

A schematic diagram of the measurement system is shown in Fig. 4. The sample is heated with a 5 W argon ion laser beam focussed on a line and the increased IR radiation from the sample surface is monitored by a simple IR line scanner consisting of a LN^{2-} cooled HgCdTe detector operating in the 8-12 µm wavelength range, a 100 Hz deflection mirror, and a germanium IR lens optimized for the wavelengths in question. The detection line of the scanner is directed parallel to the heating pattern.

The sample is fastened on a DC-motor powered rotating stage the speed of which is adjustable. The thermal image of the sample is formed when the sample rotates perpendicularly to the radial heating line. The dimensions of the imaged area were 10 cm x 2 cm and the measurement time was about 60 seconds per image. Thus the whole coating was covered by 30 partially overlapping measurements.

The entire system is controlled by a microcomputer with a 12-bit multifunction interface board. The I/O board also digitizes the data obtained from the IR detector and collects the data from the sample position sensor controlling automatically the starting points of successive measurements. The measurement data are displayed as pseudocolor images on the computer screen and the images can be enhanced by means of digital image processing with either the measurement software or commercial programs. The data can be stored on the computer hard disk and on the tape drive unit and hardcopies can be obtained with either an inexpensive ink-jet color printer or a video printer.

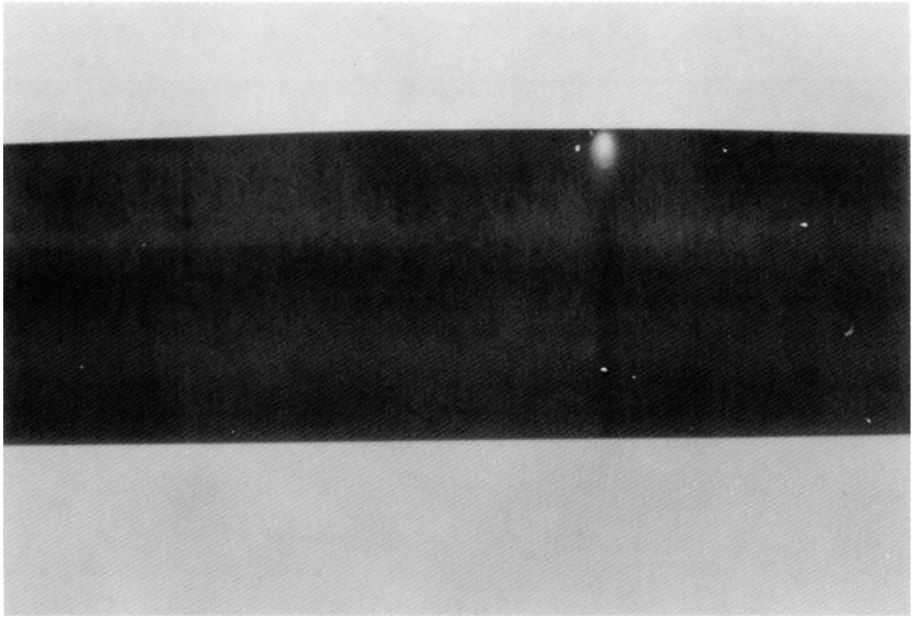

Fig. 5. A defect found from the sample. Delaminated area is discerned as a white area.

THE RESULTS

Two major adhesion defects were found in the course of the measurements. The thermal images of these faults are shown in Figures 5 and 6. The size of the first defect is 2 mm x 2 mm and the size of the second defect is 8 mm x 2 mm. Both defects are physically situated near the edge of the coating which is a probable site for adhesion failures.

CONCLUSIONS

The power of the photothermal techniques in NDE is confirmed with a practical problem of major interest. The main pump of the primary system circulates the heated and pressurized water from the reactor to steam generators and it is one of the most important components of the PWR-type nuclear power plant. Thus, it is evident that the seals of the main pump must be faultless.

The detection of clear delamination defects from the newly coated samples shows that there still exists uncontrollable parameters in the plasma-spraying techniques, which makes the thermal NDE methods worth of consideration always when dealing with the coatings of any significance.

After the photothermal inspection the sample rings are subjected to several months trial run simulating real using conditions. When the trial run is finished, the samples will be tested again in order to examine the effects of the trail run sequence, especially for the detected faulty areas of the sample, and in this way obtain new data about the connection between the detected contact resistances and the real severeness of a flaw.

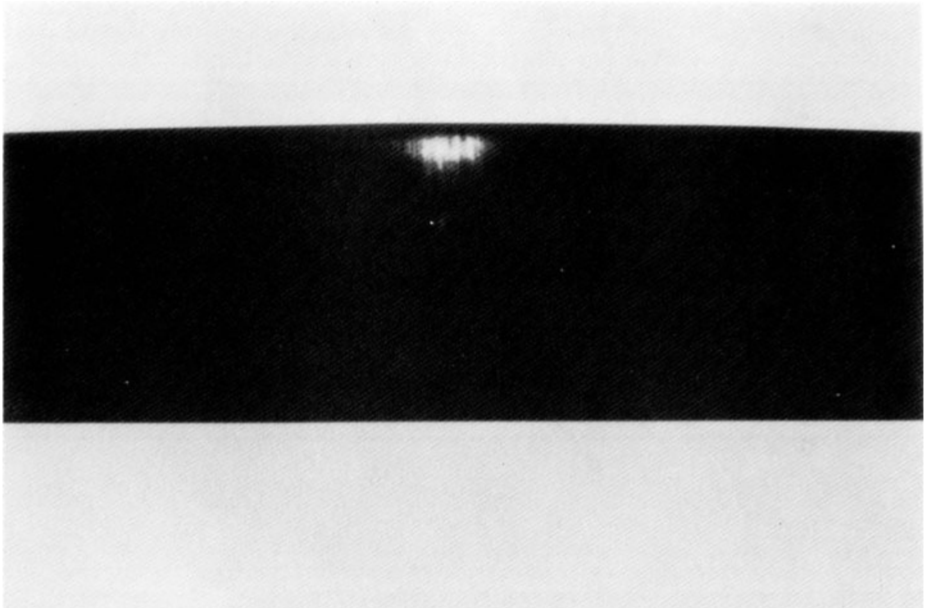

Fig. 6. An adhesion delamination defect.

REFERENCES

1. J. Hartikainen, in Review of Progress in Quantitative NDE, edited by D. O. Thompson and D. E. Chimenti (Plenum Press, New York, 1991), Vol. 9A, p. 1011.
2. J. Hartikainen, R. Lehtiniemi, and M. Luukkala, in Review of Progress in Quantitative NDE, edited by D. O. Thompson and D. E. Chimenti (Plenum Press, New York, 1991), Vol. 10A, p. 539.
3. J. Rantala, J. Hartikainen, and J. Jaarinen, Applied Physics A, 50, 465 (1990).
4. J. Hartikainen, Rev. Sci. Instr. 60, 1334 (1989).